Hindawi
Laser and Particle Beams
Volume 2021, Article ID 6616439, 6 pages
https://doi.org/10.1155/2021/6616439

CAMBRIDGE
UNIVERSITY PRESS

Research Article

Formation of H_3O^+ in the Ionization and Fragmentation of Ethanol Induced by Electron Beam Irradiation

Chao Ma,[1] **Jiaqi Zhou**,[1,2] **Enliang Wang**,[2,3] **Tao Yang**,[1] **Zhongfeng Xu**,[1] **Shaokui Jia**,[1] **Alexander Dorn**,[2] **and Xueguang Ren**[1,2]

[1]*MOE Key Laboratory for Nonequilibrium Synthesis and Modulation of Condensed Matter, School of Physics, Xi'an Jiaotong University, Xi'an 710049, China*
[2]*Max-Planck-Institut für Kernphysik, Saupfercheckweg 1, Heidelberg 69117, Germany*
[3]*J. R. Macdonald Laboratory, Department of Physics, Kansas State University, Manhattan, Kansas 66506, USA*

Correspondence should be addressed to Zhongfeng Xu; zhfxu@mail.xjtu.edu.cn and Xueguang Ren; renxueguang@xjtu.edu.cn

Received 8 October 2020; Revised 25 October 2020; Accepted 1 November 2020; Published 20 January 2021

Academic Editor: T. Shao

The single ionization and dissociation of ethanol molecules induced by low-energy electrons ($E_0 = 90$ eV) are investigated using multiparticle coincident momentum spectroscopy. By detecting two outgoing electrons (e_1 and e_2) and one fragment ion in coincidence, we obtain the energy deposition ($E_0 - E_1 - E_2$) during electron ionization of the molecule, i.e., the binding energy spectra, for production of the different ionic fragments $C_2H_5OH^+$, $C_2H_4OH^+$, COH^+, and H_3O^+. These data allow us to study the ionization channels for different ionic products. In particular, we focus on H_3O^+ as a product of double hydrogen migration. It is found that this channel mainly originates from the ionization of outer-valance orbitals ($3a''$,$10a'$, $2a''$, $9a'$, $8a'$, $1a''$, and $7a'$). Additionally, there are minor contributions from the inner-valence orbitals such as $6a'$, $5a'$, and $4a'$. Quantum chemistry calculations show two fragmentation pathways: concerted and sequential processes for formation of H_3O^+.

1. Introduction

Particle beam and laser-induced ionization and fragmentation of molecules have attracted considerable interest for several decades [1–22]. Hydrogen or proton migration is a widely existing phenomenon during these processes, and it plays a vital role in various fields of physics, chemistry, and biology [1, 2, 7, 19, 20]. In particular, for small organic molecules [3–5] or molecular complexes [6–8], the isomerization process induced by intra- and intermolecular hydrogen transfer has been extensively studied due to its high relevance, e.g., in biological processes such as in DNA mutations [9, 10]. The ultrafast hydrogen migration can unlock new dissociation channels, such as hydrogen exchange [11], scrambling [12], and roaming [13, 14]. Recent studies showed that it can also stabilize the repulsive potential energy surface of dications before the direct Coulomb explosion occurs [15].

The ethanol molecule (C_2H_5OH) contains both hydroxyl and methyl groups and is widely applied in the chemical industry as an important solvent. C_2H_5OH has attracted significant interest for studying hydrogen migration due to the relatively large number of hydrogen atoms bound to the various sites in the C-C-O skeleton. Here, of particular interest is the double hydrogen migration [23–26], forming a H_3O^+ hydronium ion, which is central in acid-catalyzed reactions as the active protonating agent. Nevertheless, the understanding of the double H migration is incomplete since it is a rather complex process involving more than one C-H bond cleavage and at least two O-H bond formations.

H_3O^+ formation has been studied by Raalte and Harrison in an electron impact ionization experiment with deuterated ethanol. Two reaction pathways were proposed, i.e., a concerted path and a sequential fragmentation path. For the concerted path, the two hydrogen migration directly follows single ionization of ethanol, while the sequential path

proceeds via the intermediate $C_2H_4OH^+$ cation where initially hydrogen is abstracted and hydrogen migration occurs subsequently [23]. Later on, Niwa et al. performed an experiment on ethanol using the photoelectron-photoion coincidence (PEPICO) technique. By analyzing the breakdown diagrams and appearance energies (AE) for the different fragment ions, they concluded that H_3O^+ was mainly formed by the sequential fragmentation [24]. Further studies using the time of flight (TOF) spectra and the quantum chemical calculations confirmed that the sequential process is the dominant pathway for the formation of H_3O^+ in ethanol [25, 26].

In this work, we study the ionization and dissociation of ethanol irradiated by low-energy electrons using an (e, 2e + ion) method [27–30] in which all three final-state particles are detected in coincidence. We use the projectile energy of 90 eV, which is close to the mean energy of secondary electrons produced by high-energy primary radiation, such as X-rays, α-rays, ?-rays, fast electron, and ion beams [31]. Here, the momentum vectors and, consequently, kinetic energies of the outgoing electrons (scattered and ejected electrons) and fragment ions are determined. The contributions of different ionized orbitals for formations of $C_2H_5OH^+$, $C_2H_4OH^+$, COH^+, and H_3O^+ cations are obtained by measuring the energy deposition in the ionization process, i.e., the binding energy (BE) spectra. The BE is defined as the energy difference between the initial projectile electron energy E_0 and the energy sum of the scattered (E_1) and ejected (E_2) electrons: $BE = E_0 - (E_1 + E_2)$. The BE resolution of $\Delta E_{BE} = 3.7$ eV, full width of half maximum (FWHM), has been achieved with a measurement on the ionization of helium. For ethanol, there are two conformers assigned as the *trans* and the *gauche* structures where the main difference is the dihedral angle between the hydroxyl and the carbon skeleton. Here, we consider the *trans* conformer with C_s symmetry as the geometric structure of ethanol [32]. The ground-state electronic structure of the valence shell can be expressed as $(4a')^2$ $(5a')^2$ $(6a')^2$ $(7a')^2$ $(1a'')^2$ $(8a')^2$ $(9a')^2$ $(2a'')^2$ $(10a')^2$ $(3a'')^2$.

2. Experiment

The experiment was performed using the multiparticle coincident momentum spectrometer (reaction microscope) combined with a pulsed electron beam [33]. The details of the experimental setup can be found in the earlier work [27, 34]; thus, only a brief introduction is given here. A well-focused (about 1 mm in diameter) electron beam with an energy of 90 eV is crossed with an ethanol gas jet. The projectile electron beam is emitted from an electron gun in which a tantalum photocathode is irradiated by a pulsed ultraviolet laser beam. The wavelength, repetition rate, and pulse width of the laser beam are 266 nm, 40 kHz, and 0.5 ns, respectively. The energy per pulse of the laser is about 1~2 nJ, and the flux of the projectile electron is about 5 nA/cm^2. The data accumulation time is about 100 hours for the present work. The gas jet is generated by the supersonic gas expansion of He (1 bar) with seeded ethanol vapor through a nozzle with a diameter of 30 μm and a two-stage differential pumping system. The ethanol gas was produced through the reservoir including the liquid ethanol at room temperature. The supersonic beam was collimated by two sequential skimmers (250 μm and 400 ?m diameter, respectively) and transmitted into the reaction area of the main chamber. After traversing the jet, the nonscattered electron beam is guided into the central hole of the electron detector as a beam dump. The charged particles in the final state (two electrons and one ion) are extracted and guided by homogeneous electric and magnetic fields towards two-dimensional position- and time-sensitive microchannel plate detectors. Three-dimensional momentum vectors of the detected particles are determined from the time-of-flight and positions of the particles hitting the detectors. The ionization process can be expressed as follows:

$$e^- + CH_3CH_2OH \rightarrow CH_3CH_2OH^+ + 2e^- \quad (1)$$

3. Quantum Chemistry Calculations

The theoretical calculations are performed utilizing the Gaussian quantum chemistry package [35]. The ground-state equilibrium geometries of the singly charged ethanol molecule, the transition states (TSs), and intermediates (INTs) are optimized by the M06-2X method with the def2TZVP basis set. The zero-point energy (ZPE) correction is acquired by the M06-2X method with the def2TZVP basis set, and the electronic energy was calculated by employing the coupled-cluster single-double and perturbative triple (CCSD(T)) method with the aug-cc-pVQZ basis set. The validity of reaction pathways is confirmed by the NBO population and the intrinsic reaction coordinate (IRC) analysis which is carried out at the M06-2X/def2TZVP level.

4. Results and Discussion

The BE spectra for the formation of the $C_2H_5OH^+$ parent ion and $C_2H_4OH^+$ with H-loss are presented in Figure 1. The experimental data for $C_2H_5OH^+$ correspond to a single peak located at about 10.8 eV, which is consistent with the ionization energy of the highest occupied molecular orbital (HOMO) of ethanol [32]. This result indicates that the $C_2H_5OH^+$ parent ion is formed through the HOMO ionization, i.e., the $3a''$ orbital of the *trans* conformer [32]. For the H-loss channel, i.e., the $C_2H_4OH^+$ cation, the measured BE spectrum shows a single peak located at about 12.6 eV which can be attributed to the ionization of the of HOMO-1 ($10a'$) plus some amount of the internal energy (~0.5 eV), leading to the subsequent H-loss.

Figure 2 presents the binding energy spectrum for the ionic fragment with a mass-to-charge (m/z) ratio of 29 u. Due to the m/z degeneracy for COH^+ and $C_2H_5^+$, we are unable to distinguish them in our experiment. Hudson and McAdoo obtained the appearance energies (AE) of about 14.2 eV for COH^+ and 12.7 eV for $C_2H_5^+$ [24] by comparing the breakdown curves for $C_2H_5OH^+$ and $C_2D_5OD^+$. The present experimental data show a peak structure centered at about 15.3 eV and a shoulder structure at higher BE, and thus, we assigned the ionic product with 29 u to COH^+ through the pathway of C-C bond breaking and two

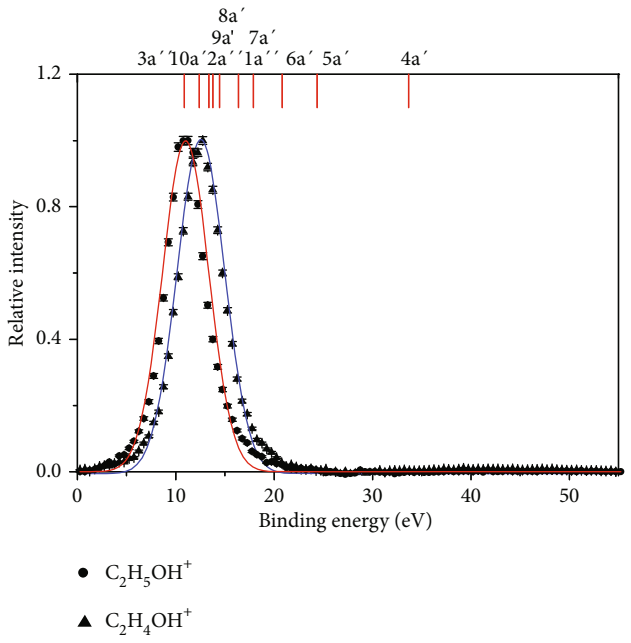

Figure 1: The binding energy spectra related to the $C_2H_5OH^+$ and $C_2H_4OH^+$ cations. The black solid circles and the black solid triangles with error bars represent the experimental data of $C_2H_5OH^+$ and $C_2H_4OH^+$, respectively. The data for both ions are normalized to unity at the maximum. The red and blue solid curves are Gaussian fits. At the top of the plot, red solid vertical lines indicate the ionization energies of valence orbitals [32].

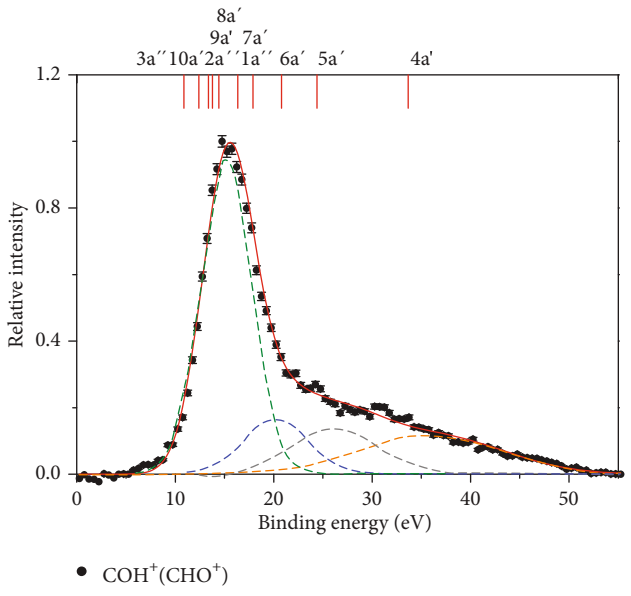

Figure 2: The binding energy spectrum for the formation of the COH^+ cation. The dashed lines are Gaussian fits, while the red solid curve is the sum of the Gaussians.

hydrogen loss from the C_α site [24]. The BE spectrum indicates that the ionization of several valence orbitals leads to the formation of COH^+. The main peak located at 15.3 eV corresponds to ionization of 10a′, 2a″, 9a′, 8a′, 1a″, and 7a′ orbitals which cannot be resolved energetically. Additionally, ionization of inner-valence orbitals (6a′, 5a′, and 4a′) can also contribute to the formation of COH^+. We determine the branching ratios of about 55% and 45% for outer-valance and inner-valence ionization, respectively. It is also to be noted that the measured peaks at higher BE, e.g., 35.8 eV, may result also from the ionization plus excitation or from multiple scattering within ethanol clusters [36].

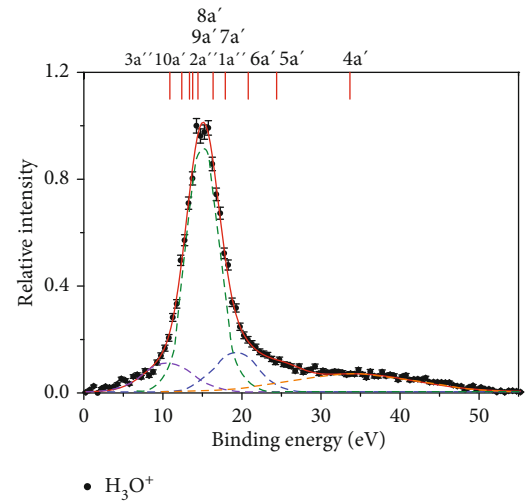

Figure 3: The same as Figure 2 but for H_3O^+.

Concerning the production pathway of COH^+, Hudson and McAdoo theoretically demonstrated a sequential process involving the H migration. First, a neutral H is ejected, and in the second step, the hydrogen transfers from hydroxyl to the methyl group, and then, the C_α-C_β bond breaks with the ejection of neutral methane [26]. The reaction process is expressed as follows:

$$\begin{aligned} CH_3CH_2OH^+ &\rightarrow CH_3CHOH^+ + H \\ CH_3CHOH^+ &\rightarrow CHO^+ + CH_4 \end{aligned} \quad (2)$$

It is considered that the CHO^+ production with H migration and the COH^+ formation without H migration are both involved in our experiment. The fragmentation channels induced by the ionization of inner-valence orbitals (6a′, 5a′, and 4a′) may be concerned with the CHO^+ formation due to the higher deposited energy supporting for H migration. We notice that the formation of CHO^+ through hydrogen transfer from oxygen to carbon is different from the widely studied H migration process in ethanol where the migrated H is originated from carbon and moves to the oxygen side [15, 23–25].

The measured BE spectrum for the formation of H_3O^+ is presented in Figure 3, which exhibits a single-peak structure centered at about 15.1 eV and a tail structure at higher BE. The peak at BE ~15.1 eV can be attributed to the ionization of 10a′, 2a″, 9a′, 8a′, and 1a″ orbitals, while the structures at higher BE are caused by the ionization of inner-valence orbitals (6a′, 5a′, and 4a′) and also the ionization plus excitation or multiple scattering processes in clusters [36]. Previous studies by Niwa et al. [24] and Shirota et al. indicate that

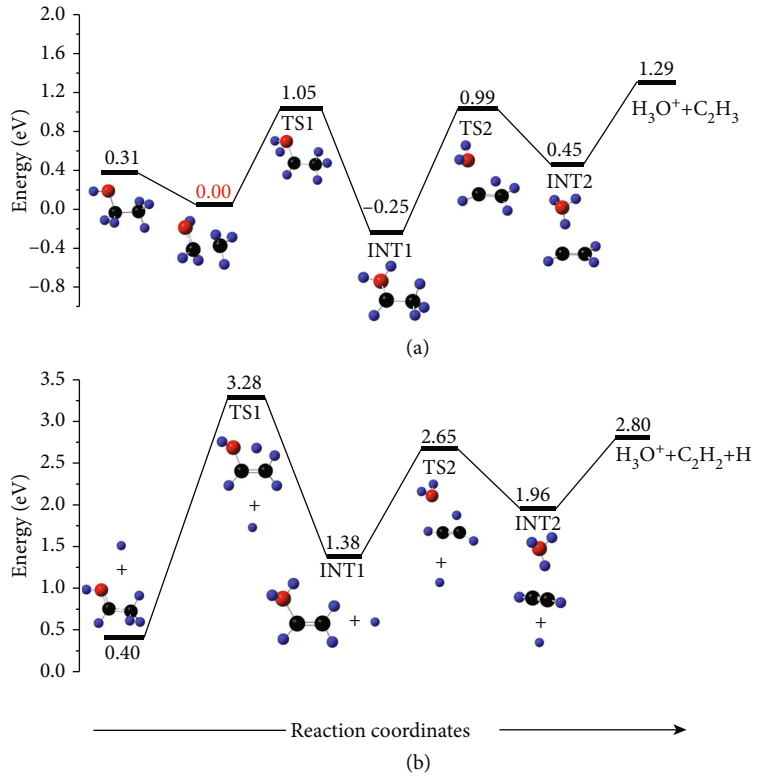

FIGURE 4: Calculated potential energy diagrams for the formation of H_3O^+ via concerted (a) and sequential (b) processes. The energy values in (a) and (b) are relative to the ionic ground state $CH_3CH_2OH^+$ (0.00 eV) in (a). The single point energy is calculated at the CCSD(T)/aug-cc-pVQZ level, and all the values include the zero-point vibrational energy corrections which are calculated with the M06-2X/def2TZVP level. The reaction pathway has been confirmed by the intrinsic reaction coordinate (IRC) calculation. The black, blue, and red balls represent carbon, hydrogen, and oxygen atoms, respectively.

the formation of H_3O^+ is dominated by the sequential process via the intermediate CH_3CHOH^+ cation. In the first step, one C_α-H bond breaks and neutral hydrogen is ejected. After that, the fragmentation of CH_3CHOH^+ produces H_3O^+. The reaction process is expressed as follows:

$$CH_3CHOH^+ \rightarrow H_3O^+ + C_2H_2 \quad (3)$$

A theoretical work [26] demonstrated a reaction pathway where the two H which migrate to form H_3O^+ originate from the methyl site and sequentially transfer to the hydroxyl site. On the other hand, recent experiments on deuterated ethanol showed a complete scrambling of the four hydrogens at the C-C site before migration to the hydroxyl site [25]. This is in agreement with an earlier study for deuterated CH_3CD_2OH which mainly shows yields of H_3O^+ and H_2DO^+ in accordance with that expected for a CH_3CDOH^+ intermediate [23]. In addition, a small yield of HD_2O^+ shows that also the direct concerted fragmentation pathway contributes where both H from the C_α site migrate:

$$CH_3CH_2OH^+ \rightarrow C_2H_3 + H_3O^+ \quad (4)$$

To trace the complete reaction pathways of double H migration processes, we performed quantum chemical calculations for H_3O^+ formation in both concerted and sequential ways. The potential energy diagrams are shown in Figure 4 which exhibits the reaction pathways with transition states (TS1 and TS2) and intermediate states (INT1 and INT2). In Figure 4, the energy values are relative to the ionic ground state of $CH_3CH_2OH^+$, which is marked by 0.0 eV in Figure 4(a). The single point energy is calculated at the CCSD(T)/aug-cc-pVQZ level including the zero-point vibrational energy corrections. The reaction pathways are confirmed by the intrinsic reaction coordinate (IRC) calculation following routes from transition state to related local minima in two directions. For the concerted pathway in Figure 4(a), the $CH_3CH_2OH^+$ doublet state (0.31 eV) is formed through a vertical transition. After relaxing to the ionic ground state (0.00 eV), the first H transfers from C_α to the hydroxyl, leading to the metastable intermediate $CH_3CHOH_2^+$ (INT1). The second H migration from the $C_?$ migrates to the -H_2O radical group via the transition state (TS2), and then, the system dissociates into the H_3O^+ cation and a neutral C_2H_3.

For the sequential pathway in Figure 4(b), the calculated potential energies are consistent with the previous studies [25, 26]. The H-loss channel occurs with the C_α-H bond cleavage in the first step that forms the CH_3CHOH^+ cation (0.4 eV). After that, the double H migration occurs subsequently from methyl to hydroxyl sites through the transition states of TS1 (3.28 eV) and TS2 (2.65 eV), and then, the system dissociates into a H_3O^+ cation and a C_2H_2 neutral fragment. Our calculation indicates that for the sequential

process, higher internal energy is needed to overcome the potential barrier (TS1: 3.28 eV) in comparison with the concerted pathway (TS1: 1.05 eV). From this point of view, the concerted pathway is more accessible. However, fast H-loss channel is expected due to its lower energy barrier (0.40 eV). This can cause the observed dominance of the sequential process [23]. Nevertheless, future studies in both experiment and theory are required to unambiguously identify the concerted pathway.

5. Conclusions

We have presented results from the first (e, 2e + ion) study of the ionization-induced dissociation of ethanol induced by low-energy electron impact (90 eV). A multiparticle coincidence momentum spectrometer is used in which all three charged final-state particles, i.e., two outgoing electrons and one fragment ion, are detected in triple coincidence. The momenta and, consequently, the kinetic energies of all three final-state particles are obtained through the measurement of their TOFs and hit positions. We determine the binding energy (BE) spectra correlated with different ionic fragments, i.e., the parent ion $C_2H_5OH^+$, the H-loss channel $C_2H_4OH^+$, and the hydrogen migration channels of COH^+ and H_3O^+ cations.

The present results confirm that the nondissociated $C_2H_5OH^+$ ion product arises due to the HOMO ($3a''$) orbital ionization, which is consistent with the results of previous appearance energy studies. The BE spectrum for the H-loss channel reveals a single-peak (12.6 eV) structure which can be assigned to the HOMO-1 ($10a'$) orbital ionization. While for COH^+ product, both the outer-valence ($10a'$, $2a''$, $9a'$, $8a'$, $1a''$, and $7a'$) and inner-valence ($6a'$, $5a'$, and $4a'$) orbital ionizations are observed from the measured BE spectrum. The BE spectrum for H_3O^+ product shows the similar feature in which the outer-valence ($3a''$, $10a'$, $2a''$, $9a'$, $8a'$, $1a''$, and $7a'$) and inner-valence ($6a'$, $5a'$, and $4a'$) orbital ionizations are involved. For the formation of H_3O^+ through double H migration, two fragmentation pathways (concerted and sequential processes) are identified using quantum chemistry calculations. The higher BE peaks can also result from the ionization plus excitation or from multiple scattering of the projectile in ethanol clusters. The present study can have implications for a better understanding of the ionization-induced isomerization mechanisms of molecules.

Data Availability

The experimental data used to support the findings of this study are available from the corresponding author upon request.

Conflicts of Interest

The authors declare that there is no conflict of interest regarding the publication of this paper.

Acknowledgments

J.Z. is grateful for the support from the China Scholarship Council (CSC). E.W. acknowledges a fellowship from the Alexander von Humboldt Foundation. This work was jointly supported by the National Natural Science Foundation of China under Grants Nos. 11875219, 11974272, and 11774281.

References

[1] T. J. Wasowicz and B. Pranszke, "Observation of the hydrogen migration in the cation-induced fragmentation of the pyridine molecules," *The Journal of Physical Chemistry. A*, vol. 120, no. 7, pp. 964–971, 2016.

[2] X. Ren, E. Wang, A. D. Skitnevskaya, A. B. Trofimov, K. Gokhberg, and A. Dorn, "Experimental evidence for ultrafast intermolecular relaxation processes in hydrated biomolecules," *Nature Physics*, vol. 14, no. 10, pp. 1062–1066, 2018.

[3] A. Hishikawa, A. Matsuda, M. Fushitani, and E. J. Takahashi, "Visualizing recurrently migrating hydrogen in acetylene dication by intense ultrashort laser pulses," *Physical Review Letters*, vol. 99, no. 25, p. 258302, 2007.

[4] S. Xu, H. Zhao, X. Zhu et al., "Dissociation of [HCCH]2+to H2 +and C2+: a benchmark reaction involving H migration, H–H combination, and C–H bond cleavage," *Physical Chemistry Chemical Physics*, vol. 20, no. 44, pp. 27725–27729, 2018.

[5] H. Xu, T. Okino, and K. Yamanouchi, "Tracing ultrafast hydrogen migration in allene in intense laser fields by triple-ion coincidence momentum imaging," *The Journal of Chemical Physics*, vol. 131, no. 15, p. 151102, 2009.

[6] Y. Ono and C. Y. Ng, "A study of the unimolecular decomposition of the (C2H2)2+ complex," *The Journal of Chemical Physics*, vol. 77, no. 6, pp. 2947–2955, 1982.

[7] S. Thrmer, M. Onk, N. Ottosson et al., "On the nature and origin of dicationic, charge-separated species formed in liquid water on X-ray irradiation," *Nature Chemistry*, vol. 5, no. 7, pp. 590–596, 2013.

[8] B. Oostenrijk, N. Walsh, J. Laksman et al., "The role of charge and proton transfer in fragmentation of hydrogen-bonded nanosystems: the breakup of ammonia clusters upon single photon multi-ionization," *Physical Chemistry Chemical Physics*, vol. 20, p. 932, 2017.

[9] O.-H. Kwon and A. H. Zewail, "Double proton transfer dynamics of model DNA base pairs in the condensed phase," *Proceedings of the National Academy of Sciences*, vol. 104, no. 21, pp. 8703–8708, 2007.

[10] Y. Zhang, K. de La Harpe, A. A. Beckstead, R. Improta, and B. Kohler, "UV-induced proton transfer between DNA strands," *Journal of the American Chemical Society*, vol. 137, no. 22, pp. 7059–7062, 2015.

[11] T. Okino, A. Watanabe, H. Xu, and K. Yamanouchi, "Ultrafast hydrogen scrambling in methylacetylene and methyl-d3-acetylene ions induced by intense laser fields," *Physical Chemistry Chemical Physics*, vol. 14, no. 30, pp. 10640–10646, 2012.

[12] R. Kanya, T. Kudou, N. Schirmel et al., "Hydrogen scrambling in ethane induced by intense laser fields: statistical analysis of coincidence events," *The Journal of Chemical Physics*, vol. 136, no. 20, p. 204309, 2012.

[13] J. Bowman and P. Houston, "Theories and simulations of roaming," *Chemical Society Reviews*, vol. 46, no. 24, pp. 7615–7624, 2017.

[14] N. Ekanayake, T. Severt, M. Nairat et al., "H 2 roaming chemistry and the formation of H 3+ from organic molecules in strong laser fields," *Nature Communications*, vol. 9, no. 1, p. 5186, 2018.

[15] E. Wang, X. Shan, L. Chen et al., "Ultrafast proton transfer dynamics on the repulsive potential of the ethanol dication: roaming-mediated isomerization versus Coulomb explosion," *The Journal of Physical Chemistry A*, vol. 124, no. 14, pp. 2785–2791, 2020.

[16] L. Li, L. Chang, L. Zhang, J. Liu, G. Chen, and J. Wen, "Development mechanism of cathode surface plasmas of high current pulsed electron beam sources for microwave irradiation generation," *Laser and Particle Beams*, vol. 30, no. 4, pp. 541–551, 2012.

[17] P. Katrk, D. H. H. Hoffmann, E. Mustafin, and I. Strak, "Experimental study of residual activity induced in aluminum targets irradiated by high-energy heavy-ion beams: a comparison of experimental data and FLUKA simulations," *Matter and Radiation at Extremes*, vol. 4, no. 5, article 055403, 2019.

[18] G. Wang, H. Yi, Y. Li et al., "Review of stopping power and Coulomb explosion for molecular ion in plasmas," *Matter and Radiation at Extremes*, vol. 3, no. 2, pp. 67–77, 2018.

[19] E. Wang, X. Ren, W. Baek, H. Rabus, T. Pfeifer, and A. Dorn, "Water acting as a catalyst for electron-driven molecular break-up of tetrahydrofuran," *Nature Communications*, vol. 11, no. 1, p. 2194, 2020.

[20] E. Alizadeh, T. M. Orlando, and L. Sanche, "Biomolecular damage induced by ionizing radiation: the direct and indirect effects of low-energy electrons on DNA," *Annual Review of Physical Chemistry*, vol. 66, no. 1, pp. 379–398, 2015.

[21] P. Graham, K. Ledingham, R. Singhal et al., *Laser and Particle Beams*, vol. 19, p. 187, 2001.

[22] H. A. Navid, E. Irani, and R. Sadighi-Bonabi, *Laser and Particle Beams*, vol. 31, p. 481, 2013.

[23] D. V. Raalte and A. G. Harrison, "Energetics and mechanism of hydronium ion formation by electron impact," *Canadian Journal of Chemistry*, vol. 41, no. 12, pp. 3118–3126, 1963.

[24] Y. Niwa, T. Nishimura, and T. Tsuchiya, "Ionic dissociation of ethanol studied by photoelectron—photoion coincidence spectroscopy," *International Journal of Mass Spectrometry and Ion Physics*, vol. 42, no. 1-2, pp. 91–99, 1982.

[25] T. Shirota, N. Mano, M. Tsuge, and K. Hoshina, "Formation of H3O+from alcohols and ethers induced by intense laser fields," *Rapid Communications in Mass Spectrometry*, vol. 24, no. 5, pp. 679–686, 2010.

[26] C. E. Hudson and D. J. McAdoo, "Theoretical characterizations of novel C2H5O+ reactions," *International Journal of Mass Spectrometry*, vol. 232, no. 1, pp. 17–24, 2004.

[27] X. Ren, T. Pflger, M. Weyland et al., "An (e, 2e + ion) study of low-energy electron-impact ionization and fragmentation of tetrahydrofuran with high mass and energy resolutions," *The Journal of Chemical Physics*, vol. 141, no. 13, p. 134314, 2014.

[28] X. Ren, T. Pflger, M. Weyland et al., "High-resolution (e, 2e + ion) study of electron-impact ionization and fragmentation of methane," *The Journal of Chemical Physics*, vol. 142, no. 17, p. 174313, 2015.

[29] K. Hossen, X. Ren, E. Wang, S. V. K. Kumar, and A. Dorn, "An (e, 2e+ ion) study of electron-impact ionization and fragmentation of tetrafluoromethane at low energies," *The European Physical Journal D*, vol. 72, no. 3, p. 43, 2018.

[30] S. Xu, X. Ma, X. Ren, and A. Senftleben, "Formation of protons from dissociative ionization of methane induced by 54 eV electrons," *Physical Review A*, vol. 83, no. 5, article 052702, 2011.

[31] S. Pimblott and J. LaVerne, "Production of low-energy electrons by ionizing radiation," *Radiation Physics and Chemistry*, vol. 76, no. 8-9, pp. 1244–1247, 2007.

[32] C. G. Ning, Z. H. Luo, and Y. R. Huang, "Investigation of the molecular conformations of ethanol using electron momentum spectroscopy," *Journal of Physics B: Atomic, Molecular and Optical Physics*, vol. 41, no. 17, article 175103, 2008.

[33] J. Ullrich, R. Moshammer, A. Dorn, R. Dörner, L. P. Schmidt, and H. Schmidt-Böcking, "Recoil-ion and electron momentum spectroscopy: reaction-microscopes," *Reports on Progress in Physics*, vol. 66, no. 9, pp. 1463–1545, 2003.

[34] X. Ren, E. Jabbour Al, A. D. Maalouf, and S. Denifl, "Direct evidence of two interatomic relaxation mechanisms in argon dimers ionized by electron impact," *Nature Communications*, vol. 7, no. 1, 2016.

[35] M. J. Frisch, G. W. Trucks, H. B. Schlegel et al., *Gaussian 16 Revision A.03*, Gaussian Inc. Wallingford CT, 2016.

[36] T. Pflüger, A. Senftleben, X. Ren, A. Dorn, and J. Ullrich, "Observation of Multiple Scattering in (e, 2 e) Experiments on Small Argon Clusters," *Physical Review Letters*, vol. 107, 2011.